arXiv:2503.06764v3 [cs.CV] 20 Mar 2025

SemHiTok: A Unified Image Tokenizer via Semantic-Guided Hierarchical Codebook for Multimodal Understanding and Generation

Zisheng Chen[1], Chunwei Wang[2], Xiuwei Chen[1],
Hang Xu[2], Jianhua Han[2],
Xiaodan Liang[1*]
[1] Sun Yat-sen University [2] Huawei Noah's Ark Lab

Abstract

*We present **SemHiTok**, a unified image **Tok**enizer via **Sem**antic-Guided **H**ierarchical codebook that provides consistent discrete feature representations for multimodal understanding and generation tasks. Recently, unified multimodal large models (MLLMs) for understanding and generation have sparked exploration within research community. Previous works attempt to train a unified image tokenizer by combining loss functions for semantic feature reconstruction and pixel reconstruction. However, due to the differing levels of features prioritized by multimodal understanding and generation tasks, joint training methods face significant challenges in achieving a good trade-off. SemHiTok addresses this challenge through Semantic-Guided Hierarchical codebook which builds texture sub-codebooks on pre-trained semantic codebook. This design decouples the training of semantic reconstruction and pixel reconstruction and equips the tokenizer with low-level texture feature extraction capability without degradation of high-level semantic feature extraction ability. Our experiments demonstrate that SemHiTok achieves excellent rFID score at* 256×256 *resolution compared to other unified tokenizers, and exhibits competitive performance on multimodal understanding and generation tasks.*

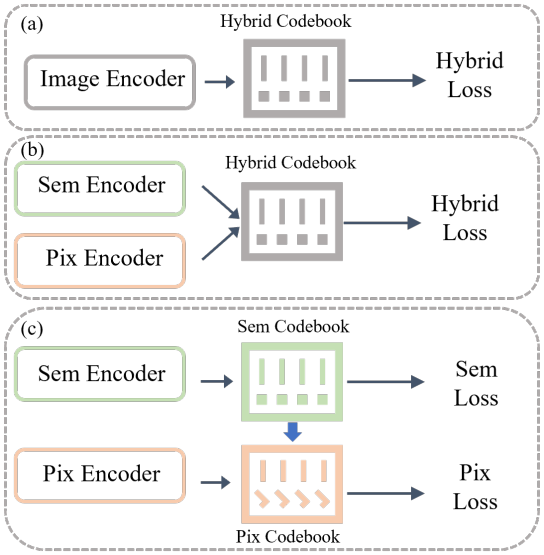


Figure 1. The joint tokenizer design paradigm is demonstrated. (a) represents the use of a single encoder, where semantic and texture information share the same discrete feature space in a jointly optimized manner; (b) represents the use of dual encoders, but the semantic and texture information still reside in the same discrete feature space; (c) represents the design paradigm of our method, using dual encoders and dual codebooks, achieving efficient unification of discrete features through unidirectional information interaction.

1. Introduction

In recent years, autoregressive models have achieved great success in natural language processing, and have been extended to the multimodal understanding domain, demonstrating immense potential. This triggers researchers' interest in unified multimodal understanding and generation by employing a single autoregressive framework. To achieve a unified multimodal large model, the key challenge is designing a tokenizer suitable for both generation and understanding tasks.

However, there is a vast gap in the visual information required for these two tasks. For instance, models from the CLIP[36, 41, 62] family, commonly used in multimodal understanding tasks, tend to lose visual texture information. On the contrary, the VQGAN[57, 66] family models, often used in autoregressive generation tasks, lack the ability to extract semantic feature for multimodal understanding. It is the core to design a unified tokenizer that simultaneously extracts textural feature and semantic feature for achieving unified MLLMs.

*Corresponding author

Recent researches combine MLLMs with diffusion models[14, 19], which introduces excessive computational. This led researchers to explore unified tokenizers. Common unified tokenizer paradigms are shown in Fig.1. VILA-U[52] and Muse-VL[55] attempt to incorporate semantic reconstruction loss during VQGAN training, aiming to derive a unified tokenizer through joint training. However, due to the gap between the two features and the optimization challenges of joint training, the model struggles to achieve a good balanced extraction of semantic and texture features. Although Janus[50] introduce a dual-encoder method that separate encoders for understanding and generation tasks to address this conflict, this increases the complexity of handling mixed tasks and does not fundamentally resolve the feature conflict challenge. TokenFlow[35] decouples semantic and pixel-level feature learning through shared mapping mechanism, whereas it does not realize a unified representation in the feature space. These limitations highlight a core challenge in the field: achieving consistent representation of semantic features and texture features, and decoupling their learning

To address this challenge, a straight forward solution is to train the semantic and texture vector quantizer separately, then concatenate quantized token either along the token length or across dimension[3]. However, this approach increases the number of tokens thereby raising computational complexity, or results in a codebook that is too large to be suitable for MLLM. Inspired by the observation that image patches with the same semantic code tend to have similar texture feature, we propose SemHiTok, a unified image tokenizer that provides consistent feature representations for multimodal understanding and generation tasks through a unique hierarchical codebook design. The crucial point is to use same discrete features for multimodal understanding and generation tasks while decoupling the learning of semantic and texture features. Through semantic-guided hierarchical codebook, we achieve a unified representation of semantic and texture features for understanding and generation task. Unlike existing approaches that directly employ a single codebook to encode different level features, SemHiTok's semantic-guided hierarchical codebook support stage-wise training paradigm where each stage exclusively optimizes specific hierarchy level features. This novel design allows us to achieve a better trade-off between semantic and texture feature extraction.

Our framework exhibits remarkable performance on multimodal understanding and generation tasks. For multimodal understanding, we surpass other next-token-based approaches using discrete visual inputs under the LLaVA-1.5 setting. SemHiTok also achieves competitive rFID metrics at a resolution of 256×256 on ImageNet. For text-to-image generation tasks, we achieve competitive results, compared existing next-token autoregressive generation methods. These findings indicate that SemHiTok achieves a better trade-off between semantic and texture feature extraction capabilities, and demonstrates the great potential for application in MLLMs.

2. Related Work

2.1. Image Tokenizer

Tokenization for Generation. Image tokenizers are crucial for autoregressive image generation[38, 44, 45]. VQVAE[45] learns a discrete representation using a learnable codebook in auto-encoder architectures. VQGAN[57] further improves better perceptual quality by using adversarial training[16]. advanced the existing architecture by integrating perceptual loss and discriminator loss, alongside adversarial loss, to enhance reconstruction quality. This approach yields more precise and detailed image representations, significantly improving upon previous methodologies in image generation and processing. Subsequently, ViT-VQGAN[58] and Efficient-VQGAN[5] advance the framework with the transformer design. In recent literature, researchers are turning to efficient codebook structures[3, 39, 58, 63] and better quantization methods[59, 61] to improve generation performance and compression rates. IBQ[39] propose the Index Backpropagation Quantization codebook update method, achieving stable training of large-scale codebooks. Although these methods efficiently retain low-level texture information, they frequently fail to capture high-level semantic information, which limits their application to multimodal understanding tasks. FQGAN[3] uses multiple codebooks and product quantization where each codebook encodes a different type of feature (Pixel, CLIP[36], DINO[6] etc.). However, this work focuses only on image reconstruction and generation tasks.

Tokenization for Understanding. In multimodal large language models (MLLMs)[1, 9, 25, 27, 30, 37], researchers leverage CLIP[37] and BLIP[25] to extract visual characteristics that align with the language during its pre-training phase. Building upon, many works[1, 9, 30] have been collected and trained on high-quality datasets to achieve remarkable performance. LLaVA[30] utilizes vision encoder to align the vision inputs before LLMs. QwenVL[1] and InterVL[9] achieve better results through increased resolution, higher-quality datasets, etc. However, these text-aligned image encoders tend to focus only on semantic information and ignore texture information, which is important for the generation task.

2.2. Unified Image Tokenizer

Numerous efforts have emerged to develop unified visual generation and understanding within one MLLM[11, 15, 42, 43, 46, 48, 53, 54]. There are two main lines to bridge the gap. Many workers[11, 15, 42] combine diffusion mod-

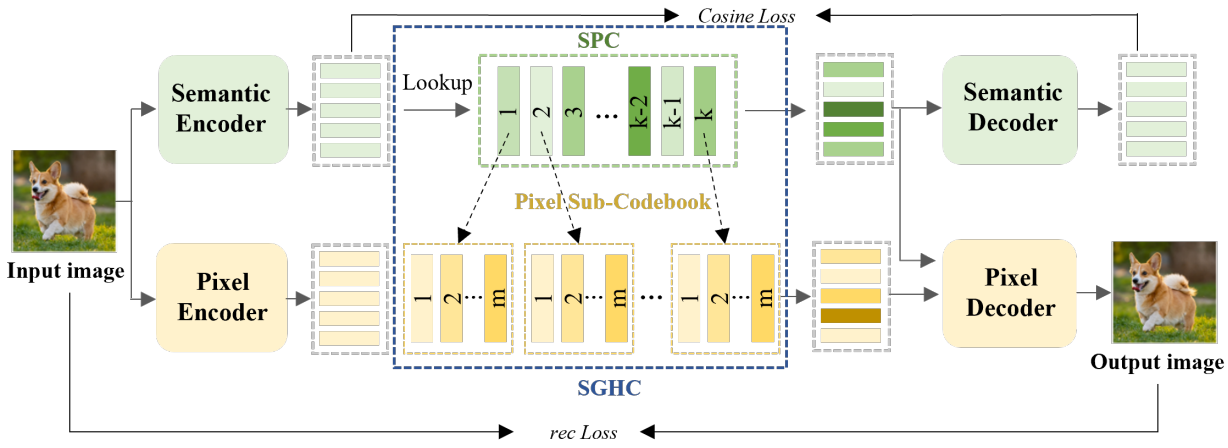


Figure 2. Overview of SemHiTok. We incorporate dual encoders and codebooks with guidance of SPC, which avoids the joint learning of semantic and texture features. Based on the pre-trained SPC, given an input image, we first perform semantic tokenization through SPC to obtain the encoded semantic codes. The image is then fed into pixel encoder to extract continuous texture features. Specifically, during texture feature quantization, the corresponding sub-pixel codebook is selected based on the spatially aligned semantic code. Finally, the quantized texture features, together with the quantized semantic features, are fed into the pixel decoder for pixel reconstruction.

els with LLMs for image generation. DREAMLLM[11] presents a unified framework that not only provides multimodal understanding but also creates multimodal content via diffusion models. Emu2[42] trains a unified generative model using a diffusion-based decoder. These approaches inevitably increase model complexity and are not simple enough. Other workers[43, 48, 53, 54] adopt VQVAE-based encoders to convert images into discrete tokens. Chameleon[43] and EMU3[48] directly use VQGAN[57], which is optimized by pixel reconstruction as the image tokenizer, while this method increases resource consumption during the pre-training stage and degrades multimodal understanding performance. VILA-U[53] introduces a unified image tokenizer that incorporates a text-aligned branch within the VQGAN training paradigm. However, due to the gap between semantic feature and texture feature, the joint optimization approach may lead to suboptimal solutions In contrast, our proposed SemHiTok can add the ability to extract texture features without changing the discrete semantic features, and avoids the challenges brought by joint optimization.

3. Method

The main objective of **SemHiTok** is to establish a simple and unified image tokenizer for understanding and generation. In this model, the image is transformed into discrete tokens that contain high-level semantic information and fine-grained texture information. We start with a Semantic-Priority Codebook(SPC) training recipe that reconstructs semantic features extracted from language image pre-training model[49, 62], and point out SPC's poor texture feature extraction capability in section 3.1. In section 3.2, we conduct a discussion on Pixel Reconstruction Enablement(PRE), and observe that the image patches corresponding to the semantic code exhibit similar texture features. Building on this observation, we introduce Semantic-Guided Hierarchical Codebook(SGHC), incorporating texture information without compromising SPC's understanding capability. Finally, we introduce the application of SemHiTok in multimodal downstream tasks in section 3.3. The overview of SemHiTok is shown in Fig.2.

3.1. Semantic-Priority Codebook Training

For multimodal understanding, use text-aligned visual encoder[36, 41, 47, 62] as image tokenizer can accelerate convergence and improve performance. However, these text-aligned visual encoder typically output continuous semantic features. In this work, to achieve a unified visual tokenizer, we first train a Semantic-Priority Codebook(SPC) to quantize the continuous semantic feature following VQKD[49].

Given an image $X^{H\times W\times 3}$, the semantic encoder $\mathcal{E}_{\text{sem}}$ extract continuous semantic features:

$$Z_{sem} = \mathcal{E}_{\text{sem}}(X) \in \mathbb{R}^{h\times w\times d_{sem}} \tag{1}$$

Where $\mathcal{E}_{\text{sem}}$ is a frozen text-aligned image encoder, *e.g.*, CLIP[36] and SigLIP[62]. Then the quantization bottleneck $\mathcal{Q}_{sem}$ transform Z_{sem} into discrete feature set space $\mathcal{C}_{sem} = \{c_1, c_2, ..., c_K\} \in \mathbb{R}^{K\times d_{sem}}$. The quantization process $\mathcal{Q}_{sem}(*)$ is as follows:

$$Z_{q_{sem}}, I_{q_{sem}} = \underset{k\in\{1,...,K\}}{\arg\min} \|Z_{sem} - \mathcal{C}_{sem}[k]\| \tag{2}$$

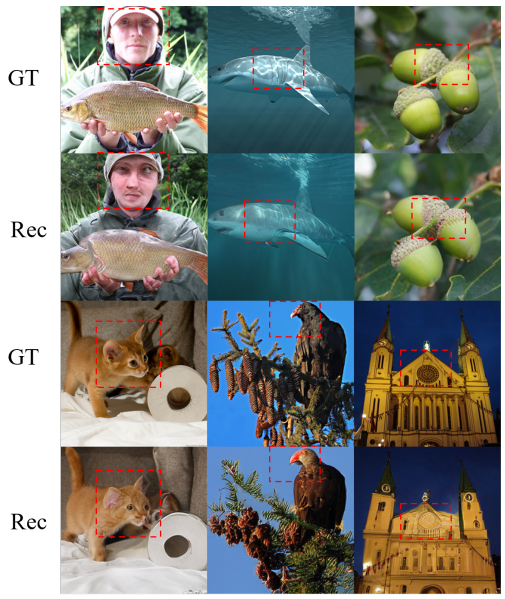


Figure 3. Visualization of reconstructed by quantized semantic features. We highlight severely erroneous regions with red dashed boxes. It is obvious that SPC's texture feature extraction capability is poor.

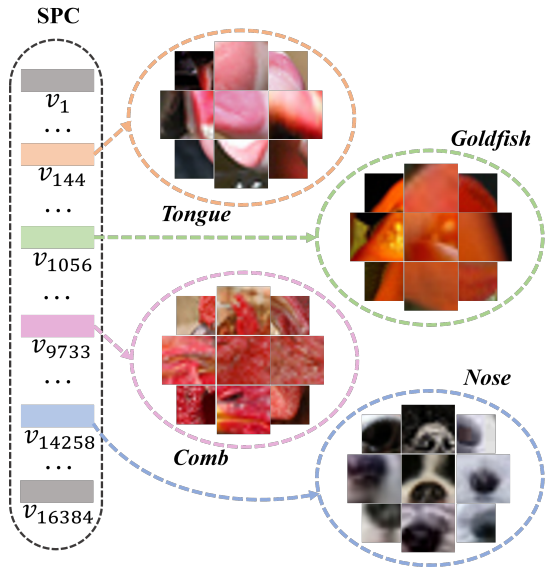


Figure 4. Visualization of the codes in SPC. We selected some image patches corresponding to certain codes, and it can be seen that the semantic codes in SPC have clear semantics concept, and the image patches corresponding to the same code exhibit similar low-level texture features.

Where $I_{q_{sem}} \in \{0, 1, \ldots, K-1\}^{h \times w}$ is quantized index, $Z_{q_{sem}} = \mathcal{C}_{sem}[I_{q_{sem}}]$ is discrete feature indexed from $\mathcal{C}_{sem}$. After quantization, semantic decoder $\mathcal{D}_{sem}$ maps $Z_{q_{sem}}$ to raw semantic feature space $\hat{Z}_{sem}$. The $\mathcal{Q}_{sem}$ and $\mathcal{D}_{sem}$ are end-to-end trainable by minimizing Cosine loss $\mathcal{L}_{cos} = 1 - \cos(Z_{q_{sem}}, \hat{Z}_{sem})$ and quantization loss $\mathcal{L}_q(Q)$.

We conduct multimodal understanding experiments using discrete features output by SPC in the LLaVA-1.5 setting as shown in Tab.4. The experiments show that SPC is slightly inferior to continuous features but still viable. However, we further conduct an experiment reconstructing the original pixel from the quantized features extracted by SPC. The reconstructed images exhibited noticeable blurriness and a significant loss of high-frequency details, as shown in Fig. 3.

3.2. Pixel Reconstruction Enablement

Discussion. In section 3.1, we demonstrate that SPC lacks the ability to extract texture information. In order to pixel reconstruction enablement and avoid a reduction of understand ability, a straightforward approach is to add an extra VQGAN[57] model. SPC extracts discrete semantic information for comprehension tasks, and VQGAN extracts discrete texture information for generative tasks, thereby avoiding the suboptimal performance brought by joint training. However, the concatenation of semantic tokens and texture tokens introduces additional challenges. There are two distinct methods of concatenation: length-wise concatenation and dimension-wise concatenation. The former approach results in an increase in the number of tokens required per image, leading to higher computational, while the latter causes the whole visual codebook size to be equal to the product of the sizes of the two codebooks, which is too large to be acceptable for LLM.

Furthermore, we present the visualization results of the semantic code, as shown in Fig.4. It can be observed that image patches corresponding to the same code exhibit similar texture features. For example, the code $\sqsubseteq_{9733}$ is more likely to be assigned to the rooster comb element in the image. At the same time, the image patches corresponding to these combs exhibit similar texture features, such as folds, patterns, and shapes Based on this observation, we propose Semantic-Guided Hierarchical Codebook to model the texture feature space corresponding to each semantic code using sub-codebook.

Semantic-Guided Hierarchical Codebook (SGHC). The SGHC consists of SPC and several sub-codebooks, where each sub-codebook corresponds to a semantic code of SPC. Specially, given the SPC's pre-trained semantic codebook $\mathcal{C}_{sem} = \{c_1, c_2, ..., c_K\} \in \mathbb{R}^{K \times d_{sem}}$, the pixel codebook $\mathcal{C}_{pix} = \{\mathcal{C}^1_{pix}, \mathcal{C}^2_{pix}, \ldots, \mathcal{C}^K_{pix}\} \in \mathbb{R}^{K \times m \times d_{pix}}$, where $\mathcal{C}^k_{pix} \in \mathbb{R}^{m \times d_{pix}}$ is k_{th} semantic code's pixel sub-codebook, m is the sub-codebook size. At first, the SPC quantizes input image X to discrete semantic token Z_{sem} and semantic codebook index I_{sem}. In parallel, pixel encoder $\mathcal{E}_{pix}$ extract continuous texture features $Z_{pix} = \mathcal{E}_{pix}(X)$. For the quantization process of the pixel codebook, the correspond-

ing pixel sub-codebook is selected based on the quantization result of the semantic codebook. For instance, given image patch i, its semantic quantization codebook index k and its continuous pixel feature Z^i_{pix}, SGHC selects pixel sub-codebook $\mathcal{C}^k_{pix}$ to quantize Z^i_{pix}. The process is as follows:

$$Z^i_{q_{pix}}, I^i_{q_{pix}} = \underset{j\in\{1,\dots,m\}}{\arg\min} \|Z^i_{pix} - \mathcal{C}^i_{pix}[j]\| \tag{3}$$

where j is selected sub-codebook internal index. Finally, the semantic quantized tokens and pixel quantized tokens are concatenated to $Z = concate_{dim}(Z_{q_{sem}}, Z_{q_{pix}})$ as the input of pixel decoder $\mathcal{D}_{pix}$ to reconstruct raw pixel image:

$$\hat{X} = \mathcal{D}_{pix}(Z) \tag{4}$$

where $\hat{X}$ is reconstructed pixel image. The $\mathcal{E}_{pix}$, C_{pix} and $\mathcal{D}_{pix}$ are end-to-end trainable by minimizing reconstruction loss $L_{img} = \ell_1(\hat{X}, X)$, codebook loss Lc, perceptual loss L_{per} and represents adversarial loss L_{gan}. The reconstruction loss is formulated as:

$$L_{rec} = L_{img} + \lambda_1 Lc + \lambda_2 L_{per} + \lambda_3 L_{gan} \tag{5}$$

where λ_1, λ_2 and λ_3 are loss weight of each item.

Our SGHC can be regarded as the refinement of semantic discrete space to enable pixel reconstruction. We place a specific emphases on two key advantage of SGHC: (1) ***Non-Conflicting Extension:*** Our method leverages a pre-trained semantic codebook as foundation, with pixel reconstruction losses exclusively employed to optimize pixel branch modules during the PRE. This strategic approach effectively circumvents the suboptimal solutions that arise from joint optimization processes. Furthermore, SGHC's final output is generated by concatenating semantic-quantized features with texture-quantized features, preserving the full expressive capacity of the original semantic features while integrating complementary texture information through this unified feature fusion paradigm. It's important to emphasize that subsequent reconstruction, multimodal understanding, and generation experiments are all conducted using discrete features derived from SGHC. (2) ***Efficient Downstream Applications:*** SGHC effectively avoids two critical predicaments: token quantity inflation and codebook over-expansion. As defined before, semantic codebook size K and each pixel sub-codebook m. Due to dimensional splicing, the complete codebook expands to $K \times m$, where m is much more smaller than K. In our experimental default settings, we extend complete codebook to a size comparable to existing LLM's vocabulary size, e.g., the size of Qwen2' vocabulary [47, 56] is 150k. Leveraging these strengths, our framework demonstrates robust performance across multimodal downstream tasks, validating the effectiveness of the proposed architectural design.

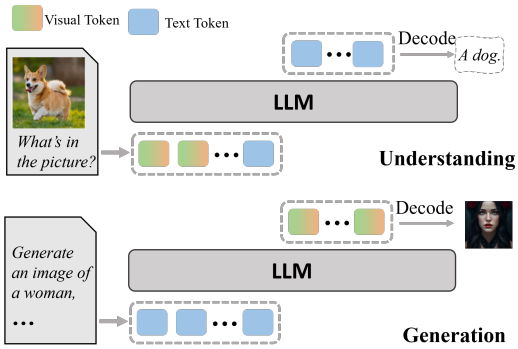


Figure 5. Framework of multimodal downstream tasks.

Type	Method	Res	Code Num	Codebook Size	rFID↓
Pixel	VQGAN[57]	256	256	16,384	4.98
	LlamaGen[40]	256	256	16,384	2.19
	RQVAE[20]	256	256[&]	16,384	3.20
	RQVAE[20]	256	1024[&]	16,384	1.30
	VQGAN-LC[66]	256	256	16,384	3.01
	VQGAN-LC[66]	256	256	100,000	2.62
	IBQ[39]	256	256	16,384	1.37
	IBQ[39]	256	256	262,144	1.00
	FQGAN[3]	256	256	$16384 \times 2^{\dagger}$	0.94
	FQGAN[3]	256	256	$16384 \times 3^{\dagger}$	0.76
Uni	VILA-U[52]	256	1024[&]	16,384	1.80
	SDE[55]	256	256	32,768	2.26
	TokenFlow[35]	256	680	32,768	1.37
	SemHiTok(ours)[*]	256	256	196,608	**1.10**
	SemHiTok(ours)	256	256	196,608	**1.24**

Table 1. Comparison of reconstruction quality on the ImageNet-50k validation set. *: model is only trained on ImageNet. [&]: quantizer uses residual quantization (RQ), where the total Code Num are multiplied by RQ depth. [†]: quantizer uses multiple codebooks and product quantization.

3.3. Multimodal Downstream Tasks

The framework diagram for multimodal downstream tasks is shown in Fig.5. We use unified discrete visual features for multimodal understanding and generation tasks **Multimodal Understanding.** SemHiTok acts as a visual VQ tokenizer, providing the LLM with quantized features containing semantic information. Following the LLaVA-1.5 paradigm, the image is passed through SemHiTok to obtain quantized visual features, which are then input to the LLM after a simple MLP layer. In order to achieve feature consistency, quantized semantic and texture features are spliced as input to LLM, and our experiments shown that there is negligible performance impact in comprehension tasks compared to direct utilization of quantized semantic features, confirming the viability of our feature integration strategy.

Visual Generation. We deploy the visual generation model on pre-trained LLM. For encoding text, we directly use

Visual Token	Method	# Params	Res.	SEEDB	POPE	GQA	MMMU	MMB	MME	MME-P
Continuous	InstructBLIP [29]	Vicuna-13B	224	58.8	78.9	49.5	50.7	36.0	–	1212.8
	MiniGPT-4 [65]	Vicuna-13B	224	–	–	–	–	–	1158.7	866.6
	BLIP-2 [26]	Vicuna-13B	224	46.4	–	–	42.5	–	–	1293.8
	ShareGPT4V [8]	Vicuna-7B	336	69.7	–	63.3	60.4	68.8	1943.8	1567.4
	NExT-GPT [51]	Vicuna-7B	224	57.5	–	–	–	58.0	–	–
	Qwen-VL-Chat [2]	Qwen-7B	448	57.7	–	57.5	–	–	1848.3	1487.5
	Janus [50]	DeepSeek-LLM-1.3B	384	63.7	87.0	59.1	30.5	69.4	–	1338.0
	LLaVA-1.5 [31]	Vicuna-13B	336	68.1	85.9	63.3	36.4	67.7	1826.7	1531.3
Discrete	LWM [32]	LLaMA-2-7B	256	–	75.2	44.8	–	–	–	–
	SEED-LLaMA [22]	LLaMA-2-13B	224	53.7	–	–	–	–	–	–
	Show-o [54]	Phi-1.5-1.3B	256	–	80.0	58.0	26.7	–	–	1097.2
	EMU3 [48]	8B from scratch	512	68.2	85.2	60.3	31.6	58.5	1509.9	1243.8
	MUSE-VL[55]	Qwen2.5-7B	256	70.0	–	–	42.3	72.1	–	1480.4
	VILA-U [52]	LLaMA-2-7B	256	56.3	83.9	58.3	–	–	–	1336.2
	VILA-U [52]	LLaMA-2-7B	384	78.7	86.8	–	–	–	–	1401.8
	TokenFLow-L [52]	Vicuna-13B	256	62.6	85.0	60.3	34.4	60.3	1622.9	1365.4
	TokenFLow-XL [52]	Vicuna-13B	384	59.0	86.8	62.7	38.7	68.9	1590.4	1401.8
	SemHiTok(ours)	Vicuna-7B	256	58.7	83.2	58.8	34	54.7	1590.4	1307.4
	SemHiTok(ours)	Vicuna-7B	384	62.4	84.2	61.0	35.2	60.3	1724.2	1400.6

Table 2. Evaluation on multimodal understanding benchmarks. We include approaches with continuous visual inputs versus discrete visual inputs. SemHiTok achieved competitive performance under the LLaVA-v1.5 setting.

LLM's BPE tokenizer to convert text into discrete token sequences. We add special visual tokens to the original vocabulary and adjust the head layer accordingly. Follow the autoregressive image generation training paradigm, we leverage SemHitok to convert images into discrete token sequences, and splice them with text token sequences for input to LLM, using the cross-entropy function to compute the loss of visual tokens. Regarding the discrete coding of vision, for example, for the j_{th} code in the i_{th} pixel sub-codebook, the discrete code index in the completed codebook is $h = i \times m + j$. To enable classifier-free guidance[17], we randomly replace the text condition with probability of 0.1 to the un-condition text during training.

4. Experiments

4.1. Experimental Setup

Datasets. The training of SemHiTok is conducted in two stages. During SPC training, we train the semantic tokenizer for one epoch on 50M subset of COYO-700M[4]. For PRE stage, we first trained the model on ImageNet[10], and then fine-tune on 50M COYO-700M subset to improve its generalization, following LlamaGen[40]. To further improve the reconstruction and generation performance, we enlarge the size of the pixel decoder and fine-tune it on the same data. For multimodel understanding, we train VLM on LLaVA-Pretrain558K and LLaVA-v1.5-mix-665K. To evaluate the performance of the VLM, we test the model on vision-language benchmarks such as SEEDB: SEED-Image[21], POPE[28], MMMU[60], MMB[33], MME-P: MME-Perception[13] and MME[13]. We run the evaluation based on lmms-eval[64]. For visual generation with SemHiTok, we use 15M in-house text-image pairs,and evaluate on GenAI[23] and MJHQ30K[24].

Implement Details. For SPC, we employ SigLIP[62] as the semantic encoder and update semantic codebook using EMA[18] algorithm to enhance stability. We use SigLIP-large-p16 and SigLIP-so400m-p14 as semantic encoder for 256×256 and 384×384 resolution, respectively. We set semantic codebook size is 16384. The semantic decoder comprises three self-attention layers[12]. In the pixel branch, we first use ViT-Base as the pixel encoder and decoder, then increase the pixel decoder to a ViT-Large in the fine-tuning enhanced decoder stage. The default pixel sub-codebook size is 12, so the whole codebook size is 196608. For multimodal downstream tasks, we use Vicuna-v1.5-7B[30] and Qwen2.5-3B[1] as the language model for multimodal understanding tasks and generation tasks, respectively. During image generation inference, we apply classifier-free guidance[17], with a scale factor of 2.

4.2. Unified Image Tokenizer

We present reconstruction performance of SemHiTok on ImageNet-50k validation set at 256×256 resolutions and $16\times$ compression ratio in Tab.1. The * indicates that model is only trained on ImageNet, which is the same as the expert pixel reconstruction. In an ImageNet-only training setting, SemHiTok achieves 1.10 rFID, which outperforms the most of pixel-expert models, such as LlamaGen and RQ-VAE. Notably, compared to IBQ which has close codebook size to ours, SemHiTok is only higher by 0.1.

Compared with the unified tokenizer, SemHiTok

achieves **1.24** rFID which is state-of-the-art performance. These results demonstrate the effectiveness of our SGHC design scheme. In the subsequent multimodal understanding experiments and visual generation experiments, we use the model in the last column as the image tokenizer.

Model	Params	Res.	GenAI-Bench Basic ↑	GenAI-Bench Advanced ↑	MJHQ30K gFID ↓
PixArt-α [7]	0.6B	1024	–	–	6.14
SDXL [34]	2.6B	1024	0.83	0.63	9.55
LWM [32]	7B	256	0.63	0.53	17.77
Show-o [54]	1.5B	256	0.70	0.60	15.18
VILA-U [52]	7B	256	0.76	0.64	12.81
VILA-U [52]	7B	384	0.73	0.61	7.69
ILLUME [52]	7B	512	0.75	0.60	7.76
Janus [50]	1.3B	384	–	–	9.55
SemHiTok(ours)	3B	256	0.74	0.58	9.4

Table 3. Comparison of generation quality on GenAI [23] and MJHQ30K [24].

4.3. Multimodal Understanding

We present the performance of VLMs using SemHiTok's encoder on vision-language benchmarks in Tab. 2. VLMs are classified into two categories based on whether the input visual token is discrete: continuous visual tokens and discrete visual tokens. Compared to VLMs based on continuous tokens, LLMs utilizing discrete tokens generally exhibit lower performance. Among LLMs with discrete tokens, SemHiTok achieves competitive performance despite being trained on a smaller dataset and built upon a old-fashioned base model. To be specifically, compared to LWM, which employs a traditional VQVAE and uses same size LLM as ours, SemHiTok significantly outperforms it across all metrics. Additionally, when compared to VILA-U, which also adopts a unified tokenizer, SemHiTok achieves comparable performance. Our experiments demonstrate that SemHiTok effectively achieves a satisfactory trade-off between semantic and texture information.

4.4. Text-to-Image Generation

The results of SemHiTok on the text-to-image generation task are shown in Tab. 3. On GenAI, SemHiTok demonstrates competitive performance under basic and advanced prompts. This indicates that our generation model is able to be aligned to complex prompt words. We attribute this to the powerful text feature extraction capabilities of the Qwen2.5 LLM, as well as the SGHC, which contains semantic information and can efficiently align the text feature space. On the MJHQ30K, our model achieved 9.4 gFID and also demonstrated competitive performance, exceeds show-o and VILA-U under same resolution. In Fig. 6, we present some generated images from MJHQ30K. Our model also demonstrates consistency with the text on MJHQ30K, even with long prompts. Owing to the powerful reconstruction capabilities of SemHiTok, the generated images are rich in detail and highly realistic, such as the fur of human and animal, the texture of leaves, and so on.

SemEnc Init.	Texture Incorp.	SGHC.	rFID ↓	GQA ↑	POPE ↑	SEEDB ↑
			3.10	56.7	80.4	54.1
✔			2.73	58.2	83.1	57.4
✔	✔		2.10	58.0	77.3	56.7
✔	✔	✔	**1.24**	**58.8**	**83.2**	**58.7**

Table 4. Impact of key design choices on reconstruction quality and multimodal understanding benchmarks. The bolded parts represent the best results.

4.5. Ablation

Impact of Key Design. In Tab.4, we validate the impact of our key design choices in SemHiTok: initialization for the semantic encoder, incorporation of texture features, semantic-guided hierarchical codebook(SGHC). The baseline experimental setup involves training SPC with a randomly initialized semantic encoder. Incorporation of texture features refers to the joint training of texture information based on SPC, following the setup of MUSE-VL[55].

Our experiments indicate that initialization for the semantic encode with a teacher model significantly enhances the model's understanding performance. Meanwhile, the semantic tokenizer that only considers semantic information fails to effectively capture the texture information for reconstruction. Furthermore, although a simple joint training approach improves rFID reduced by **0.63**, it leads to a decline in understanding performance which is non-negligible. Finally, with the introduction of the SGHC design, not only is reconstruction performance improved, but understanding ability is also preserved without degradation. These experiments highlight the core advantage of the SGHC, which enables the incorporation of texture feature extraction without compromising the understanding ability of the semantic tokenizer.

Impact of Fusion Type and Sub-Codebook Size. For efficiency, we only conduct training and evaluation on ImageNet. We experiment to investigate the impact of the fusion type of semantic and pixel discrete features, as well as the sub-codebook size, on reconstruction performance as shown in Tab. 5. The gray bar represents the default setting in our experiments. For fusion type, experiments show that concatenation along the dimension yields the best performance. In contrast, the reconstruction performance without semantic discrete token is the worst, indicating that semantic information can be used as supplementary information to improve the reconstruction. Due to semantic discrete tokens correspond to texture discrete tokens in 2D grid space, the concatenation fusion type in the length direction is not appropriate. For sub-codebook size, increasing the size can improve the model's reconstruction performance, but it ex-

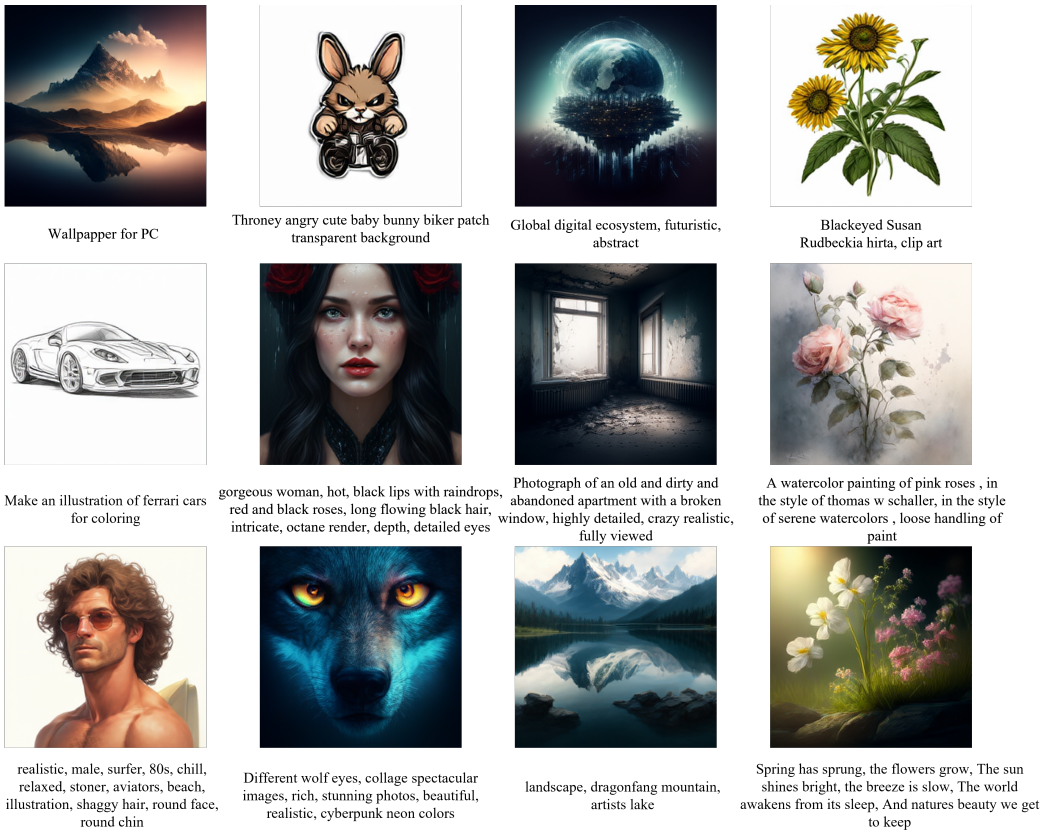


Figure 6. Presentation of the generated results at a resolution of 256×256 on MJHQ30K. Our generated images show good consistency with the prompts in terms of objects and style

Fusion	Subc Size	rFID ↓	Usage↑
w/o sem	12	1.99	98.4%
Len	12	1.45	97.1%
Dim	8	1.42	96.4%
	12	1.26	93.7%
	16	1.19	79.3%

Table 5. Impact of fusion type and sub-codebook size. w/o sem: not use semantic discrete token. Len: concatenate in length direction. Dim: concatenate in dimension direction

hibits marginal utility. In addition, the codebook usage significantly decreases when the sub-codebook size is set to 16, which indicates that too large a sub-codebook size is not cost-effective.

5. Conclusion

In this work, we introduce SemHiTok, a unified image tokenizer that implements better trade-off between high-level and low-level semantic information. SemHiTok innovatively utilizes semanitc-guied hierarchical codebook to realize the reconstruction capability of texture features without affecting the understanding performance of the original semantic codebook, and achieves SOTA at ImageNet 256×256 resolution. We conducted extensive experiments on multimodal understanding tasks and generation tasks, and SemHiTok achieves competitive performance with a small amount of data. These results verify the powerful unified multimodal capability of SemHiTok, and provide an effective solution for understanding and generating integrated multimodal large models.

Limitation In this work, we primarily focus on pixel reconstruction enablement without any degeneration in understanding performance based on the existing semantic codebook, without extensively exploring the design of the semantic codebook. In addition, we mainly conducted experiments on multimodal downstream tasks at a resolution of 256×256, and further exploration is needed to assess performance variations at higher resolutions.

Future Work In the future, we can explore more efficient training methods and advance codebook structure for semantic tokenizer to bridge the gap between discrete and continuous features in multimodal tasks.

References

[1] Jinze Bai, Shuai Bai, Shusheng Yang, Shijie Wang, Sinan Tan, Peng Wang, Junyang Lin, Chang Zhou, and Jingren Zhou. Qwen-vl: A frontier large vision-language model with versatile abilities. *ArXiv*, abs/2308.12966, 2023. 2, 6

[2] Jinze Bai, Shuai Bai, Shusheng Yang, Shijie Wang, Sinan Tan, Peng Wang, Junyang Lin, Chang Zhou, and Jingren Zhou. Qwen-vl: A frontier large vision-language model with versatile abilities. *arXiv preprint arXiv:2308.12966*, 1(2):3, 2023. 6

[3] Zechen Bai, Jianxiong Gao, Ziteng Gao, Pichao Wang, Zheng Zhang, Tong He, and Mike Zheng Shou. Factorized visual tokenization and generation. *arXiv preprint arXiv:2411.16681*, 2024. 2, 5

[4] Minwoo Byeon, Beomhee Park, Haecheon Kim, Sungjun Lee, Woonhyuk Baek, and Saehoon Kim. Coyo-700m: Image-text pair dataset, 2022. 6

[5] Shiyue Cao, Yueqin Yin, Lianghua Huang, Yu Liu, Xin Zhao, Deli Zhao, and Kaigi Huang. Efficient-vqgan: Towards high-resolution image generation with efficient vision transformers. In *Proceedings of the IEEE/CVF International Conference on Computer Vision*, pages 7368–7377, 2023. 2

[6] Mathilde Caron, Hugo Touvron, Ishan Misra, Hervé Jégou, Julien Mairal, Piotr Bojanowski, and Armand Joulin. Emerging properties in self-supervised vision transformers. In *Proceedings of the IEEE/CVF international conference on computer vision*, pages 9650–9660, 2021. 2

[7] Junsong Chen, Jincheng Yu, Chongjian Ge, Lewei Yao, Enze Xie, Yue Wu, Zhongdao Wang, James Kwok, Ping Luo, Huchuan Lu, et al. Pixart-alpha: Fast training of diffusion transformer for photorealistic text-to-image synthesis. *arXiv preprint arXiv:2310.00426*, 2023. 7

[8] Lin Chen, Jinsong Li, Xiaoyi Dong, Pan Zhang, Conghui He, Jiaqi Wang, Feng Zhao, and Dahua Lin. Sharegpt4v: Improving large multi-modal models with better captions. In *European Conference on Computer Vision*, pages 370–387. Springer, 2024. 6

[9] Zhe Chen, Jiannan Wu, Wenhai Wang, Weijie Su, Guo Chen, Sen Xing, Muyan Zhong, Qinglong Zhang, Xizhou Zhu, Lewei Lu, et al. Internvl: Scaling up vision foundation models and aligning for generic visual-linguistic tasks. In *Proceedings of the IEEE/CVF conference on computer vision and pattern recognition*, pages 24185–24198, 2024. 2

[10] Jia Deng, Wei Dong, Richard Socher, Li-Jia Li, Kai Li, and Li Fei-Fei. Imagenet: A large-scale hierarchical image database. In *2009 IEEE conference on computer vision and pattern recognition*, pages 248–255. Ieee, 2009. 6

[11] Runpei Dong, Chunrui Han, Yuang Peng, Zekun Qi, Zheng Ge, Jinrong Yang, Liang Zhao, Jianjian Sun, Hongyu Zhou, Haoran Wei, et al. Dreamllm: Synergistic multimodal comprehension and creation. *arXiv preprint arXiv:2309.11499*, 2023. 2, 3

[12] Alexey Dosovitskiy, Lucas Beyer, Alexander Kolesnikov, Dirk Weissenborn, Xiaohua Zhai, Thomas Unterthiner, Mostafa Dehghani, Matthias Minderer, Georg Heigold, Sylvain Gelly, et al. An image is worth 16x16 words: Transformers for image recognition at scale. *arXiv preprint arXiv:2010.11929*, 2020. 6

[13] Chaoyou Fu, Peixian Chen, Yunhang Shen, Yulei Qin, Mengdan Zhang, Xu Lin, Jinrui Yang, Xiawu Zheng, Ke Li, Xing Sun, et al. Mme: A comprehensive evaluation benchmark for multimodal large language models. *arXiv preprint arXiv:2306.13394*, 2023. 6

[14] Yuying Ge, Sijie Zhao, Ziyun Zeng, Yixiao Ge, Chen Li, Xintao Wang, and Ying Shan. Making llama see and draw with seed tokenizer. *arXiv preprint arXiv:2310.01218*, 2023. 2

[15] Yuying Ge, Sijie Zhao, Jinguo Zhu, Yixiao Ge, Kun Yi, Lin Song, Chen Li, Xiaohan Ding, and Ying Shan. Seed-x: Multimodal models with unified multi-granularity comprehension and generation. *arXiv preprint arXiv:2404.14396*, 2024. 2

[16] Ian Goodfellow, Jean Pouget-Abadie, Mehdi Mirza, Bing Xu, David Warde-Farley, Sherjil Ozair, Aaron Courville, and Yoshua Bengio. Generative adversarial nets. *Advances in neural information processing systems*, 27, 2014. 2

[17] Jonathan Ho and Tim Salimans. Classifier-free diffusion guidance. *arXiv preprint arXiv:2207.12598*, 2022. 6

[18] J Stuart Hunter. The exponentially weighted moving average. *Journal of quality technology*, 18(4):203–210, 1986. 6

[19] Yang Jin, Kun Xu, Liwei Chen, Chao Liao, Jianchao Tan, Quzhe Huang, Bin Chen, Chenyi Lei, An Liu, Chengru Song, et al. Unified language-vision pretraining in llm with dynamic discrete visual tokenization. *arXiv preprint arXiv:2309.04669*, 2023. 2

[20] Doyup Lee, Chiheon Kim, Saehoon Kim, Minsu Cho, and Wook-Shin Han. Autoregressive image generation using residual quantization. In *Proceedings of the IEEE/CVF Conference on Computer Vision and Pattern Recognition*, pages 11523–11532, 2022. 5

[21] Bohao Li, Rui Wang, Guangzhi Wang, Yuying Ge, Yixiao Ge, and Ying Shan. Seed-bench: Benchmarking multimodal llms with generative comprehension. *arXiv preprint arXiv:2307.16125*, 2023. 6

[22] Bohao Li, Yuying Ge, Yixiao Ge, Guangzhi Wang, Rui Wang, Ruimao Zhang, and Ying Shan. Seed-bench: Benchmarking multimodal large language models. In *Proceedings of the IEEE/CVF Conference on Computer Vision and Pattern Recognition*, pages 13299–13308, 2024. 6

[23] Baiqi Li, Zhiqiu Lin, Deepak Pathak, Jiayao Li, Yixin Fei, Kewen Wu, Tiffany Ling, Xide Xia, Pengchuan Zhang, Graham Neubig, et al. Genai-bench: Evaluating and improving compositional text-to-visual generation. *arXiv preprint arXiv:2406.13743*, 2024. 6, 7

[24] Daiqing Li, Aleks Kamko, Ehsan Akhgari, Ali Sabet, Linmiao Xu, and Suhail Doshi. Playground v2. 5: Three insights towards enhancing aesthetic quality in text-to-image generation. *arXiv preprint arXiv:2402.17245*, 2024. 6, 7

[25] Junnan Li, Dongxu Li, Caiming Xiong, and Steven Hoi. Blip: Bootstrapping language-image pre-training for unified vision-language understanding and generation. In *International conference on machine learning*, pages 12888–12900. PMLR, 2022. 2

[26] Junnan Li, Dongxu Li, Silvio Savarese, and Steven Hoi. Blip-2: Bootstrapping language-image pre-training with frozen image encoders and large language models. In *International conference on machine learning*, pages 19730–19742. PMLR, 2023. 6

[27] Junnan Li, Dongxu Li, Silvio Savarese, and Steven Hoi. Blip-2: Bootstrapping language-image pre-training with frozen image encoders and large language models. In *International conference on machine learning*, pages 19730–19742. PMLR, 2023. 2

[28] Yifan Li, Yifan Du, Kun Zhou, Jinpeng Wang, Wayne Xin Zhao, and Ji-Rong Wen. Evaluating object hallucination in large vision-language models. *arXiv preprint arXiv:2305.10355*, 2023. 6

[29] Haotian Liu, Chunyuan Li, Qingyang Wu, and Yong Jae Lee. Visual instruction tuning. *Advances in neural information processing systems*, 36:34892–34916, 2023. 6

[30] Haotian Liu, Chunyuan Li, Qingyang Wu, and Yong Jae Lee. Visual instruction tuning. *Advances in neural information processing systems*, 36:34892–34916, 2023. 2, 6

[31] Haotian Liu, Chunyuan Li, Qingyang Wu, and Yong Jae Lee. Visual instruction tuning. *Advances in neural information processing systems*, 36:34892–34916, 2023. 6

[32] Hao Liu, Wilson Yan, Matei Zaharia, and Pieter Abbeel. World model on million-length video and language with ringattention. *arXiv e-prints*, pages arXiv–2402, 2024. 6, 7

[33] Yuan Liu, Haodong Duan, Yuanhan Zhang, Bo Li, Songyang Zhang, Wangbo Zhao, Yike Yuan, Jiaqi Wang, Conghui He, Ziwei Liu, et al. Mmbench: Is your multi-modal model an all-around player? In *European conference on computer vision*, pages 216–233. Springer, 2024. 6

[34] Dustin Podell, Zion English, Kyle Lacey, Andreas Blattmann, Tim Dockhorn, Jonas Müller, Joe Penna, and Robin Rombach. Sdxl: Improving latent diffusion models for high-resolution image synthesis. *arXiv preprint arXiv:2307.01952*, 2023. 7

[35] Liao Qu, Huichao Zhang, Yiheng Liu, Xu Wang, Yi Jiang, Yiming Gao, Hu Ye, Daniel K Du, Zehuan Yuan, and Xinglong Wu. Tokenflow: Unified image tokenizer for multimodal understanding and generation. *arXiv preprint arXiv:2412.03069*, 2024. 2, 5

[36] Alec Radford, Jong Wook Kim, Chris Hallacy, Aditya Ramesh, Gabriel Goh, Sandhini Agarwal, Girish Sastry, Amanda Askell, Pamela Mishkin, Jack Clark, et al. Learning transferable visual models from natural language supervision. In *International conference on machine learning*, pages 8748–8763. PmLR, 2021. 1, 2, 3

[37] Alec Radford, Jong Wook Kim, Chris Hallacy, Aditya Ramesh, Gabriel Goh, Sandhini Agarwal, Girish Sastry, Amanda Askell, Pamela Mishkin, Jack Clark, et al. Learning transferable visual models from natural language supervision. In *International conference on machine learning*, pages 8748–8763. PmLR, 2021. 2

[38] Robin Rombach, Andreas Blattmann, Dominik Lorenz, Patrick Esser, and Björn Ommer. High-resolution image synthesis with latent diffusion models. In *Proceedings of the IEEE/CVF conference on computer vision and pattern recognition*, pages 10684–10695, 2022. 2

[39] Fengyuan Shi, Zhuoyan Luo, Yixiao Ge, Yujiu Yang, Ying Shan, and Limin Wang. Taming scalable visual tokenizer for autoregressive image generation. *arXiv preprint arXiv:2412.02692*, 2024. 2, 5

[40] Peize Sun, Yi Jiang, Shoufa Chen, Shilong Zhang, Bingyue Peng, Ping Luo, and Zehuan Yuan. Autoregressive model beats diffusion: Llama for scalable image generation. *arXiv preprint arXiv:2406.06525*, 2024. 5, 6

[41] Quan Sun, Yuxin Fang, Ledell Wu, Xinlong Wang, and Yue Cao. Eva-clip: Improved training techniques for clip at scale. *arXiv preprint arXiv:2303.15389*, 2023. 1, 3

[42] Quan Sun, Yufeng Cui, Xiaosong Zhang, Fan Zhang, Qiying Yu, Yueze Wang, Yongming Rao, Jingjing Liu, Tiejun Huang, and Xinlong Wang. Generative multimodal models are in-context learners. In *Proceedings of the IEEE/CVF Conference on Computer Vision and Pattern Recognition*, pages 14398–14409, 2024. 2, 3

[43] Chameleon Team. Chameleon: Mixed-modal early-fusion foundation models. *arXiv preprint arXiv:2405.09818*, 2024. 2, 3

[44] Keyu Tian, Yi Jiang, Zehuan Yuan, Bingyue Peng, and Liwei Wang. Visual autoregressive modeling: Scalable image generation via next-scale prediction. *Advances in neural information processing systems*, 37:84839–84865, 2025. 2

[45] Aaron Van Den Oord, Oriol Vinyals, et al. Neural discrete representation learning. *Advances in neural information processing systems*, 30, 2017. 2

[46] Chunwei Wang, Guansong Lu, Junwei Yang, Runhui Huang, Jianhua Han, Lu Hou, Wei Zhang, and Hang Xu. Illume: Illuminating your llms to see, draw, and self-enhance. *arXiv preprint arXiv:2412.06673*, 2024. 2

[47] Peng Wang, Shuai Bai, Sinan Tan, Shijie Wang, Zhihao Fan, Jinze Bai, Keqin Chen, Xuejing Liu, Jialin Wang, Wenbin Ge, et al. Qwen2-vl: Enhancing vision-language model's perception of the world at any resolution. *arXiv preprint arXiv:2409.12191*, 2024. 3, 5

[48] Xinlong Wang, Xiaosong Zhang, Zhengxiong Luo, Quan Sun, Yufeng Cui, Jinsheng Wang, Fan Zhang, Yueze Wang, Zhen Li, Qiying Yu, et al. Emu3: Next-token prediction is all you need. *arXiv preprint arXiv:2409.18869*, 2024. 2, 3, 6

[49] Chen Wei, Haoqi Fan, Saining Xie, Chao-Yuan Wu, Alan Yuille, and Christoph Feichtenhofer. Masked feature prediction for self-supervised visual pre-training. In *Proceedings of the IEEE/CVF conference on computer vision and pattern recognition*, pages 14668–14678, 2022. 3

[50] Chengyue Wu, Xiaokang Chen, Zhiyu Wu, Yiyang Ma, Xingchao Liu, Zizheng Pan, Wen Liu, Zhenda Xie, Xingkai Yu, Chong Ruan, et al. Janus: Decoupling visual encoding for unified multimodal understanding and generation. *arXiv preprint arXiv:2410.13848*, 2024. 2, 6, 7

[51] Shengqiong Wu, Hao Fei, Leigang Qu, Wei Ji, and Tat-Seng Chua. Next-gpt: Any-to-any multimodal llm. In *Forty-first International Conference on Machine Learning*, 2024. 6

[52] Yecheng Wu, Zhuoyang Zhang, Junyu Chen, Haotian Tang, Dacheng Li, Yunhao Fang, Ligeng Zhu, Enze Xie, Hongxu

Yin, Li Yi, et al. Vila-u: a unified foundation model integrating visual understanding and generation. *arXiv preprint arXiv:2409.04429*, 2024. 2, 5, 6, 7

[53] Yecheng Wu, Zhuoyang Zhang, Junyu Chen, Haotian Tang, Dacheng Li, Yunhao Fang, Ligeng Zhu, Enze Xie, Hongxu Yin, Li Yi, et al. Vila-u: a unified foundation model integrating visual understanding and generation. *arXiv preprint arXiv:2409.04429*, 2024. 2, 3

[54] Jinheng Xie, Weijia Mao, Zechen Bai, David Junhao Zhang, Weihao Wang, Kevin Qinghong Lin, Yuchao Gu, Zhijie Chen, Zhenheng Yang, and Mike Zheng Shou. Show-o: One single transformer to unify multimodal understanding and generation. *arXiv preprint arXiv:2408.12528*, 2024. 2, 3, 6, 7

[55] Rongchang Xie, Chen Du, Ping Song, and Chang Liu. Muse-vl: Modeling unified vlm through semantic discrete encoding. *arXiv preprint arXiv:2411.17762*, 2024. 2, 5, 6, 7

[56] An Yang, Baosong Yang, Beichen Zhang, Binyuan Hui, Bo Zheng, Bowen Yu, Chengyuan Li, Dayiheng Liu, Fei Huang, Haoran Wei, et al. Qwen2. 5 technical report. *arXiv preprint arXiv:2412.15115*, 2024. 5

[57] Jiahui Yu, Xin Li, Jing Yu Koh, Han Zhang, Ruoming Pang, James Qin, Alexander Ku, Yuanzhong Xu, Jason Baldridge, and Yonghui Wu. Vector-quantized image modeling with improved vqgan. *arXiv preprint arXiv:2110.04627*, 2021. 1, 2, 3, 4, 5

[58] Jiahui Yu, Xin Li, Jing Yu Koh, Han Zhang, Ruoming Pang, James Qin, Alexander Ku, Yuanzhong Xu, Jason Baldridge, and Yonghui Wu. Vector-quantized image modeling with improved vqgan. *arXiv preprint arXiv:2110.04627*, 2021. 2

[59] Qihang Yu, Mark Weber, Xueqing Deng, Xiaohui Shen, Daniel Cremers, and Liang-Chieh Chen. An image is worth 32 tokens for reconstruction and generation. *Advances in Neural Information Processing Systems*, 37:128940–128966, 2025. 2

[60] Xiang Yue, Yuansheng Ni, Kai Zhang, Tianyu Zheng, Ruoqi Liu, Ge Zhang, Samuel Stevens, Dongfu Jiang, Weiming Ren, Yuxuan Sun, et al. Mmmu: A massive multi-discipline multimodal understanding and reasoning benchmark for expert agi. In *Proceedings of the IEEE/CVF Conference on Computer Vision and Pattern Recognition*, pages 9556–9567, 2024. 6

[61] Kaiwen Zha, Lijun Yu, Alireza Fathi, David A Ross, Cordelia Schmid, Dina Katabi, and Xiuye Gu. Language-guided image tokenization for generation. *arXiv preprint arXiv:2412.05796*, 2024. 2

[62] Xiaohua Zhai, Basil Mustafa, Alexander Kolesnikov, and Lucas Beyer. Sigmoid loss for language image pre-training. In *Proceedings of the IEEE/CVF international conference on computer vision*, pages 11975–11986, 2023. 1, 3, 6

[63] Jiahui Zhang, Fangneng Zhan, Christian Theobalt, and Shijian Lu. Regularized vector quantization for tokenized image synthesis. In *Proceedings of the IEEE/CVF Conference on Computer Vision and Pattern Recognition*, pages 18467–18476, 2023. 2

[64] Kaichen Zhang, Bo Li, Peiyuan Zhang, Fanyi Pu, Joshua Adrian Cahyono, Kairui Hu, Shuai Liu, Yuanhan Zhang, Jingkang Yang, Chunyuan Li, and Ziwei Liu. Lmms-eval: Reality check on the evaluation of large multimodal models, 2024. 6

[65] Deyao Zhu, Jun Chen, Xiaoqian Shen, Xiang Li, and Mohamed Elhoseiny. Minigpt-4: Enhancing vision-language understanding with advanced large language models. *arXiv preprint arXiv:2304.10592*, 2023. 6

[66] Lei Zhu, Fangyun Wei, Yanye Lu, and Dong Chen. Scaling the codebook size of vqgan to 100,000 with a utilization rate of 99%. *arXiv preprint arXiv:2406.11837*, 2024. 1, 5